

1 **UNTARGETED CLASSIFICATION FOR PAPRIKA POWDER AUTHENTICATION**
2 **USING VISIBLE – NEAR INFRARED SPECTROSCOPY (VIS-NIRS)**

3 Olga Monago-Maraña^{a*}, Carl Emil Eskildsen^a, Teresa Galeano-Díaz^{b,c}, Arsenio Muñoz de la
4 Peña^{b,c}, Jens Petter Wold^a

5 ^aNofima AS – Norwegian Institute of Food, Fisheries and Aquaculture Research, PB 210, N-
6 1431, Ås, Norway

7 ^bDepartment of Analytical Chemistry, University of Extremadura, Badajoz 06006, Spain

8 ^cResearch Institute on Water, Climate Change and Sustainability (IACYS), University of
9 Extremadura, Badajoz 06006, Spain

10

11 *corresponding author. E-mail: olgamonago@gmail.com

Abstract

This paper describes a non-destructive screening method for authentication of paprika belonging to the Spanish Protected Designation of Origin (PDO) “*Pimentón de La Vera*”. Different multivariate classification models were developed in order to differentiate PDO and non-PDO samples, using visible-near infrared spectra as fingerprint for each paprika sample. Sample treatment was not required. Principal component analysis (PCA) was applied in different spectral ranges: 400 - 2500, 400 - 800 and 800 - 2500 nm. In all spectral ranges, PCA was largely able to differentiate PDO from non-PDO samples. Partial least-squares - discriminant analysis (PLS-DA), PCA-linear discriminant analysis (LDA) and PCA-quadratic discriminant analysis (QDA) were used as classification methods in the different spectral ranges. All methods were able to differentiate PDO from non-PDO samples, with error rates (ER) lower than 0.15. The best models were those obtained with PLS-DA in the NIR range (800 - 2500 nm), showing ERs lower than 0.07 and error indexes (I_{ERROR}) (false positives) lower than 0.05.

Keywords: Protected Designation of Origin (PDO); paprika; authentication; Visible-Near Infrared Spectroscopy (Vis-NIRS); multivariate analysis

1 **1. Introduction**

2 Paprika powder is used as a spice in many countries. In Spain, there are three traded types of
3 paprika, which differ in their drying process (air, sun and smoke drying). Air-dried paprika, using
4 heated air, is produced mainly in the south-east and central-east of Spain (Murcia), where the high
5 temperature conditions allow peppers to undergo rapid dehydration. Sun-dried paprika are
6 imported from South America and South Africa. Smoked paprika originates from La Vera region,
7 Extremadura in the south-west of Spain. Here, a traditional drying process is used, where oak logs
8 are burnt to heat the paprika to 40 °C and give it a smoked flavor (Martín et al., 2017).

9 Smoked paprika is recognized under the quality seal Protected Designation of Origin (PDO)
10 “*Pimentón de La Vera*” by the European Union since 2006 (Unión Europea, 2006). This product
11 is considered a high-quality product obtained by drying the fruit of autochthonous varieties of
12 peppers (*Capsicum annum L.*). Moreover, the traditional drying process confers the paprika its
13 aroma, flavor, and color (Martín et al., 2017). Adulteration of smoked paprika “*Pimentón de La*
14 *Vera*” with foreign paprika of lower quality, primarily to increase profit margins, has been a
15 concern for many years to the smoked paprika industry (Hernández, Martín, Aranda, Bartolomé,
16 & Córdoba, 2007). Therefore, inexpensive and high throughput screening tools to differentiate
17 paprika based on origin is interesting for the industry.

18 Recent reviews show how spectroscopic techniques, including near-infrared spectroscopy
19 (NIRS), can be used for detection of adulteration in herbs and spices (Kucharska-Ambrożej &
20 Karpinska, 2020; Marciano M. Oliveira, Cruz-Tirado, & Barbin, 2019). However, not many
21 studies about paprika powder adulteration were found. In the case of paprika or related products,
22 NIRS has been mainly used for quantification. For example, to quantify ASTA color, moisture
23 (Bae, Han, & Hong, 1998), capsaicinoids (Lim, Kim, Mo, & Kim, 2015; Park et al., 2008), arsenic
24 and lead (Moros et al., 2008), soluble solids content (SSC), firmness of peppers (Penchaiya,
25 Bobelyn, Verlinden, Nicolaï, & Saeys, 2009) and mycotoxins (Hernández-Hierro, García-
26 Villanova, & González-Martín, 2008). In addition, Vis-NIRS combined with multivariate
27 analysis has been used to determine total carotenoids, chlorophylls, as well as maturity stage of

28 intact peppers (Timea Ignat et al., 2013) and ascorbic acid (T. Ignat, Schmilovitch, Fefoldi,
29 Steiner, & Alkalai-Tuvia, 2012). Few works about the adulteration and/or authentication of
30 paprika powder using NIRS as analytical technique have been found in the literature. A recent
31 work about this topic was based on the detection of adulterants such as potato starch, annatto and
32 acacia gum in paprika powder samples from Spain (n = 3) and Brazil (n = 2) (M. M. Oliveira,
33 Cruz-Tirado, Roque, Teófilo, & Barbin, 2020). Detection and quantification of adulterants was
34 done using a portable NIR instrument in combination with partial least squares (PLS) regression
35 and PLS-Discriminant Analysis (PLS-DA). The results were promising with a specificity greater
36 than 90% and error rate lower than 2 % for the PLS-DA models.

37 In another study, paprika samples were clustered based on origin using NIRS and Principal
38 Component Analysis (PCA) (Molnár et al., 2018). However, only six paprika samples from Spain
39 were included in the analysis, and PDO specifications were not taken into account.

40 Only few studies have investigated the possibility of differencing between paprika samples
41 belonging to the PDO "*Pimentón de La Vera*" and samples not belonging to the PDO.
42 Discrimination has been based on color measurements with visible spectrophotometry, being
43 samples, belonging to the PDO "*Pimentón de La Vera*" or not, correctly grouped in two groups
44 with PCA (Monago Maraña, Bartolomé García, & Galeano Díaz, 2016). Then, samples were
45 classified as different PDOs ("*Pimentón de La Vera*" or "*Pimentón de Murcia*") with
46 classification efficiencies ranging from 92 to 95 % when visible spectra and multilayer
47 perceptrons artificial neural networks (MLP-ANN) were used (A. Palacios-Morillo, Jurado,
48 Alcázar, & Pablos, 2016).

49 Regarding to destructive methods, liquid chromatography has been widely used for the paprika
50 authentication. Classification and authentication have been done with different Spanish PDOs,
51 "*Pimentón de La Vera*", "*Pimentón de Murcia*", and Czech Republic paprika samples without
52 PDO. Employing ultra-high-performance liquid chromatography coupled with high-resolution
53 mass spectrometry (UHPLC-HRMS), samples were discriminated on a non-target way (Barbosa,
54 Saurina, Puignou, & Núñez, 2020) and based on the polyphenolic and capsaicinoid

55 (Barbosa, Saurina, & Oscar, 2020) with classification results of 100%. On the other hand, HPLC-
56 UV was used to obtain the phenolic profile of paprika for their authentication, confirming that
57 was enough to discriminate between PDOs (Cetó, Sánchez, Serrano, Díaz-Cruz, & Núñez, 2020).
58 Also, the presence or absence of sub-products from the smoking process (Polycyclic Aromatic
59 Hydrocarbons, PAHs) (Monago-Maraña, Galeano-Díaz, & Muñoz de la Peña, 2017),
60 hydrophobic proteins (Hernández et al., 2007) or metallic content (Ana Palacios-Morillo, Jurado,
61 Alcázar, & De Pablos, 2014) have allowed differentiation of paprika at different conditions.
62 Although being very selective, discriminating on these compounds requires sample extraction
63 steps, which normally is time consuming. For this reason, high throughput screening methods are
64 interesting for practical use in the paprika industries.

65 In this study, Vis-NIR measurements will be used, which are cost effective, high throughput and
66 non-destructive, to discriminate paprika powder samples belonging to the PDO "*Pimentón de La*
67 *Vera*" from paprika powder samples not belonging to the PDO. To achieve this goal, we use
68 multivariate qualitative analytical methods for authenticating the PDO "*Pimentón de La Vera*"
69 paprika powder samples. Different methods for classification of multivariate data were compared
70 and ranked.

71 **2. Material and methods**

72 **2.1. Samples**

73 A total of 49 paprika powder samples under the PDO "*Pimentón de La Vera*" were included in
74 the study. These samples were from five different producers and were made over a period of ten
75 years (2010 – 2020). Samples from 2010 to 2017 were obtained in 2017 (n = 35) from producers
76 and measured in that year. Samples from 2017 – 2020 (n = 14) were acquired in Spanish markets
77 in 2020 and measured that year. The samples were made under smoked conditions, following the
78 traditional process from La Vera, in Extremadura, Spain. Among these samples, there were sweet,
79 sweet/hot and hot paprika samples.

80 A total of 50 samples not belonging to any PDO were acquired from different markets in Spain
81 and Norway. Samples acquired in Norway (n = 9) were bought and measured in 2017, but samples
82 acquired in Spanish markets (n = 23) were acquired in 2017 and 2020 (n = 18), and measured the
83 corresponding year of acquisition. The production processes of these samples are unknown as
84 well as the peppers used for their production due to the fact that it is not mandatory to include
85 that information in labels of paprika samples. Among these samples, there were sweet and hot
86 paprika samples.

87 **2.2. Spectroscopic acquisition**

88 The VIS-NIRS measurements were obtained in reflectance mode using a FOSS NIRS Systems
89 XDS Rapid Content™ Analyzer (FOSS Analytical A/S, Hillerød, Denmark). In order to
90 obey *Beer's law*, the NIR spectra were transformed from reflectance (R) units into absorbance-
91 like units ($\log(1/R)$). An internal ceramic standard was used as reference. Spectra were obtained
92 from 400 to 2500 nm, with a resolution of 0.5 nm. Paprika powder samples were measured in
93 circular sample cups of approximately 79 cm² (FOSS Analytical A/S, Hillerød, Denmark).
94 Spectra from each sample were acquired in triplicate, mixing the powder for obtaining different
95 surfaces each time to obtain a representative sample spectrum. The average spectrum was used
96 for further analysis.

97 **2.3. Data processing and multivariate analysis**

98 **2.3.1. Principal component analysis**

99 Principal component analysis (PCA) was applied to explore the main variation over samples.
100 During PCA all samples were included. Prior to PCA the spectral measurements were
101 preprocessed by extended multiplicative signal corrected (EMSC) (Martens & Stark, 1991) and
102 mean centered variable-wise.

103 The objective of PCA is to compress the data, reducing it from the high dimensional variable
104 space into a lower dimensional principal component space. Each new principal component (PC)
105 is a linear combination of the original variables. The loadings describe the direction of each

106 principal component in the original X-space and the scores are the projections of the original data
107 onto the loading vectors (Wold, Esbensen, & Geladi, 1987).

108 PCAs was performed separately for the entire spectral range, the visible range (from 400 to 800
109 nm) and the NIR (800 - 2500 nm) range.

110 **2.3.2. Classification analysis**

111 For the classificatory analysis, samples were divided in two sets (training and test).
112 Approximately 60 % of the samples were used for training and the remaining 40 % of the samples
113 were used for validation. Hence, the training set was composed by 59 samples (29 PDO and 30
114 non-PDO) and the test set was formed by 40 samples (20 PDO and 20 non-PDO). The split of
115 samples was based on the recently published EuroLab Guide (TR No 01/2015, 2015), which
116 recommends a minimum of 20 samples for each class in the test sets. The training and test samples
117 were randomly chosen. Hence, this division was performed three times, and three different
118 training and test sets were obtained and used for building different calibration models. As a result,
119 the average results of three training and test sets were given with the corresponding standard
120 deviation.

121 The following classification algorithms were tested for discrimination of the sample spectra:
122 discriminant partial least-squares (PLS-DA) (Barker & Rayens, 2003), linear discriminant
123 analysis based on the PC scores of the spectra (PCA-LDA) (Mohanty, John, Manmatha, & Rath,
124 2013), and quadratic discriminant analysis based on the PC scores of the spectra (PCA-QDA)
125 (Tharwat, 2016).

126 PLS-DA involves performing a multivariate regression model to establish class limits and placing
127 a numeric value to each object/sample first, and then classifying them into a specific class. As in
128 PLS regression, the relation between instrumental response in X (spectra) and y (class coding) is
129 established, and the optimal number of latent variables is chosen based on the error range by
130 cross-validation.

131 To apply LDA or QDA, it is necessary to reduce the dimensionality of the spectral data. For that
132 PCA is used. After PCA, LDA is used when the decision line between the two groups can be
133 represented by a linear function. However, if a curved line is needed to separate the groups, then
134 QDA is more effective.

135 Prior to classification the spectral training data were preprocessed by EMSC and variable-wise
136 mean centered. Classification models were fitted on the training set using full-cross validation to
137 determine the optimal models. Then the models were tested with the external test set (pre-
138 processed with the EMSC model obtained for training previously). Data analysis was done using
139 a graphical interface (Ballabio & Consonni, 2013) in Matlab (R2016b, The MathWorks, Inc.,
140 Natick, MA, USA).

141 **2.3.3. Evaluation of the methodology**

142 In order to evaluate the screening methodology, the confusion matrices were obtained and the
143 performance parameters such as precision (PREC), sensitivity (SENS), error rate (ER), accuracy
144 (ACCU) and specificity (SPEC) were calculated.

145 The PREC is defined as the number of samples correctly assigned as belonging to the PDO (i.e.
146 true positives (TP)) over the total number of samples assigned as belonging to the PDO (i.e. the
147 total number of true positives and false positives (FP)) (Eq. 1). The SENS is the number of true
148 positives over the total number of samples belonging to the PDO (i.e. the total number of true
149 positives and false negatives (FN)) (Eq. 2). The ER is the number of samples incorrectly classified
150 by the model (i.e. the total number of false positives and false negatives) over the total number of
151 samples (Eq. 3). The ACCU is the number of samples correctly classified by the model (i.e. the
152 total number of true positives and true negatives (TN)) over the total number of samples (Eq. 4).
153 The SPEC is the number of samples correctly assigned as not belonging to the PDO (i.e. true
154 negatives) over the total number of samples not belonging to the PDO (Eq. 5).

$$155 \quad PREC = \frac{TP}{TP+FP} \quad (1)$$

$$156 \quad SENS = \frac{TP}{TP+FN} \quad (2)$$

157 $ER = \frac{FN + FP}{TP + TN + FP + FN}$ (3)

158 $ACCU = \frac{TP + TN}{TP + TN + FP + FN}$ (4)

159 $SPEC = \frac{TN}{TN + FP}$ (5)

160 Where TP and TN are the number true positive and number of true negative, respectively, and FN
161 and FP are the number of false negative and number of false positive, respectively.

162 Furthermore, two recently proposed indexes, error index (I_{ERROR}) and loss index (I_{LOSS}), for
163 assigning a specification-based quality grade for a PDO label are calculated (Cuadros-Rodríguez,
164 Valverde-Som, Jiménez-Carvelo, & Delgado-Aguilar, 2020).

165 I_{ERROR} is the probability of a sample being incorrectly assigned to the PDO class (Eq. 6). I_{LOSS} is
166 the probability of obtaining false negatives and thus the risk of economic loss due to assignment
167 error.

168 $I_{ERROR} = \frac{FP}{TP + TN + FP + FN}$ (6)

169 $I_{LOSS} = \frac{FN}{TP + TN + FP + FN}$ (7)

170 3. Results and discussion

171 3.1. VIS-NIRS spectral profiling

172 Figure 1A shows the mean of the absorption spectra for both classes (PDO and non-PDO). The
173 mean spectrum of non-PDO shows higher intensity over the whole spectral range as compared
174 with the mean spectrum for PDO. More subtle differences can be seen after pre-processing by
175 EMSC (Figure 1B). The main difference in the visible range was observed at 670 nm, and in the
176 NIR range at 1450, 1940, 2305, 2346 and 2490 nm. The visible range was previously reported to
177 be useful for the quantification of total carotenoids and chlorophylls in intact bell pepper (Timea
178 Ignat et al., 2013). In the case of NIR bands, some of them might be due to water peaks (1450 and
179 1940 nm) and the other three main peaks (2305, 2350 and 2490 nm) do most likely originate from
180 fat (Núñez-Sánchez et al., 2016).

181 3.2. Exploratory analysis

182 In order to study the most important spectral variation for discriminating PDO and non-PDO
183 samples, detect potential outliers and systematic artifacts in the samples, PCA was performed on
184 the EMSC pre-processed spectra. All 99 samples were included in the analysis. As described
185 above, PCAs were performed on different spectral ranges.

186 When including the whole spectral range, the first three principal components (PCs) explain 84
187 % of the total variation in the data set. The first principal component (PC1) explains 50 % of the
188 variation, and the corresponding loading plot (not shown) reveals the most important peaks at
189 approximately 480 and 600 nm in the visible range and at 1450 and 1940 nm in the NIR range
190 (water peaks). However, this component does not differentiate PDO from non-PDO paprika
191 samples.

192 The best discrimination is observed for scores of PC3 and PC5, explaining 12 and 4 % of the total
193 variation, respectively (Figure 2A). Clearly, two groups are established according to PDO and
194 non-PDO samples. However, the two groups are slightly overlapping. PC3 provides the clearest
195 discrimination of the groups. The clear unsupervised clustering is a good basis for supervised
196 classification.

197 The loadings for PC3 and PC5 are presented in Figure 2B. The main variables affecting the
198 separation of the groups were 540 and 670 nm in the visible range and water peaks in the NIR
199 range (Figure 2A). Score values for PC3 are generally high for the PDO samples, which means
200 that positive loadings, representing certain chemical components, are positively related to PDO
201 samples. The negative loadings observed at 1720 and 1760 nm are related with first overtone C-
202 H stretching vibration of methyl (-CH₃), methylene (-CH₂) and ethenyl (-CH=CH-) groups. The
203 loadings close to 1725 nm has been related to oleic acid and the band close to 1760 nm to saturated
204 components. The bands at 2305 and 2350 nm have previously been assigned to combination of
205 C-H stretches and deformations (Núñez-Sánchez et al., 2016; Pérez-Juan et al., 2010). Also, the
206 small band at 1207 nm is related with fat. All bands related to fat are negative loadings, suggesting
207 a relatively low concentration of fat in PDO samples.

208 Scores for PCA in the visible spectral range are presented in Figure 2C. PC4, explaining 6 % of
209 the variance, discriminates quite well between the two groups. Note that the overlap of the groups
210 is stronger when using only the visible range, compared to using the whole range. The main
211 variables affecting the clustering are those mentioned before (570 and 670 nm) as seen in the
212 loading for PC4 (Figure 2D).

213 Finally, for the NIR range, a quite good grouping of the samples is obtained in PC2 (Figure 2E)
214 due to variables corresponding to water and fat peaks. Interestingly, some peaks are more
215 pronounced in the loadings in this case. These peaks can be attributed to proteins bands: 2056 nm
216 (N-H stretching vibrations) and 2478 nm (-C-N-C stretching first overtone).

217 **3.2. Classificatory analysis**

218 As detailed in the section 2.4.2, samples were divided into training and test sets. This step was
219 performed three times and the classification model was obtained for each case. Average results
220 for confusion matrices from different sets and the corresponding validation parameters are shown
221 in Tables 1 and 2, respectively. The numbers in parentheses correspond with the standard
222 deviations from the three sets assayed.

223 For PLS-DA, the best classification results were obtained for the NIR range in both training and
224 test samples. The ERs obtained for this range were overall lower than for other ranges.
225 Interestingly, from a quality-point of view, the I_{ERROR} was lower for the NIR spectral range as
226 compared with the other spectral ranges, for both the training set and test set. This is important
227 for avoiding non-PDO samples being classified as PDO samples. The visible range gave slightly
228 less correct classifications than the whole range, but all models provided acceptable results, with
229 ERs lower than 0.11 and I_{ERROR} lower than 0.10. According to (Cuadros-Rodríguez et al., 2020),
230 a good screening method should offer an I_{ERROR} equal to or lower than 0.1 in order to minimize
231 the false-compliance error. Hence, the best choice with PLS-DA would be with the NIR range,
232 although in some cases that means that some samples would be false-negative and refused
233 categorized as PDO (PDO samples categorized as non-PDO samples).

234 Regarding the other performance parameters, SENS and SPEC present similar values (Table 2),
235 mainly in the NIR range. This means that the error is balanced, and there is not a clear trend in
236 the models for false positives, or vice versa. PREC values were higher for the NIR range, which
237 means that false positives were lower in these models, as observed in the I_{ERROR} values as well.

238 The regression coefficients for each spectral range (Figure 3) were evaluated in order to elucidate
239 the main variables contributing to the classification. For the visible range, the main variables were
240 570 and 670 nm with negative values, and 540 nm with positive value. It might be expected that
241 the variation in the visible range would be related to total carotenoids, ASTA values (extractable
242 color), as other authors reported (A. Palacios-Morillo et al., 2016). In these samples, the ASTA
243 value was not so relevant since some PDO samples were old and therefore had low ASTA values
244 (between 25 - 70). Therefore, it was expected that some samples were incorrectly classified when
245 using the visible range. However, acceptable results for classification were obtained due to other
246 variables, not related to total carotenoids. The VIP scores (not shown) were also investigated.
247 Similar information was retrieved from the VIP scores and the regression vectors (Figure 3).

248 The absorption around 670 nm has previously been related with chlorophylls (Timea Ignat et al.,
249 2013) and could be also related with pheophytins formed from chlorophylls during ripening or
250 drying process (Bonaccorsi et al., 2016) . This peak has negative regression coefficients (Figure
251 3A and 3B), which suggests that non-PDO samples have lower content of chlorophyll compared
252 to PDO samples. This is also observed in Figure 1B.

253 Regarding the NIR range, the regression coefficient positive wavelength bands associated with
254 fat, such as, 1725, 2305, 2350 and 2490 nm, again suggesting a relatively high fat content in non-
255 PDO samples. A higher fat content can have different reasons. Different types of peppers used
256 for paprika production vary in the fatty acid composition depending on genotype and
257 environmental factors. Kim et al., 2019 recently reported this for some varieties of peppers and
258 this could be extended to other kind of peppers (Kim et al., 2019). Another reason may be related
259 with the addition of sunflower vegetal oil to give stronger brightness of the powder. In the case
260 of PDO “*Pimentón de La Vera*” the amount of oil is limited to 3 % (w/w) (Unión Europea, 2006).

261 However, there are not specifications reported about other kind of paprika samples, which are not
262 under the PDO. This could mean that other paprika samples contain a higher percentage of
263 sunflower oil to give more brightness. A third reason could be related to the addition of seeds
264 from peppers used in the paprika production, which would influence in the fatty acid composition.
265 This kind of addition is not allowed in PDO samples (Unión Europea, 2006).

266 PCA-LDA and PCA-QDA gave results in accordance with PLS-DA; better results were obtained
267 when the NIR range or whole range were used to classify samples, giving ERs lower than 0.15
268 and I_{ERROR} lower than 0.11. Another important result was that PCA-QDA offered better results
269 than PCA-LDA in all cases. In the case of PCA-LDA and PCA-QDA, PREC, SENS and SPEC
270 values were slightly better for the NIR range. As in previous case, SENS and SPEC values were
271 similar, which proved that errors did not follow a clear trend.

272 Finally, it must be highlighted that these good results were obtained for three training/test sets,
273 which proved the robustness of the methods. To our knowledge, this is the first work where non-
274 destructive classification of PDO "*Pimentón de La Vera*" has been performed. The method is
275 easy and quick to use and could with some more development contribute to effective control in
276 the paprika industries.

277 **4. Conclusions**

278 Vis-NIR spectroscopy with different multivariate classification techniques have been proven to
279 discriminate between paprika samples belonging to the PDO "*Pimentón de La Vera*" and other
280 paprika samples. The variability of samples and the random choice of samples for training and
281 test, indicate that the models are quite robust. The visible range offered the good classification
282 due to chlorophylls or pheophytin compounds and NIR range showed slightly better classification
283 based on differences in absorbance of fat. PLS-DA offered somewhat better results than other
284 classification methods. It can be highlighted that all methods offered acceptable ERs and I_{ERROR} ,
285 always lower than 0.15 and 0.11, respectively. This method is easy, rapid and non-destructive,
286 being an advantage in order to implement the method for industrial purposes.

287

288 **Acknowledgements**

289 Olga Monago Maraña thanks to the Fundación Ramón Areces for a postdoctoral fellowship for
290 studies abroad in the field of Life and Matter Sciences (XXXI edition of grants, 2019/2020) to
291 support her postdoctoral studies at Nofima, Ås, Norway.

292 Financial support was provided by the Junta de Extremadura (Ayuda GR18041-Research Group-
293 FQM003 and Project IB16058) and Ministerio de Ciencia, Innovación y Universidades of Spain
294 (Project CTQ2017-82496-P), both co-financed by the Fondo Social Europeo funds. Funding was
295 also given by Norwegian Agricultural Food Research Foundation through the project
296 FoodSMaCK – Spectroscopy, Modelling & Consumer Knowledge, No. 262308 /F40.

297

298 **References**

- 299 Bae, M.-J., Han, E.-S., & Hong, S.-H. (1998). Use of near infrared spectroscopy in quality
300 control of red pepper powder. *Journal of Near Infrared Spectroscopy*, 6, A333–
301 A337.
- 302 Ballabio, D., & Consonni, V. (2013). Classification tools in chemistry. Part 1: linear
303 models. PLS-DA. *Analytical Methods*, 5, 3790–3978.
- 304 Barbosa, S., Saurina, J., & Oscar, N. (2020). Capsaicinoid profiling for the chemometric
305 characterization and classification of Paprika with Protected Designation of
306 Origin (PDO) attributes. *Molecules*, 25, 1–16.
- 307 Barbosa, S., Saurina, J., Puignou, L., & Núñez, O. (2020). Classification and
308 authentication of paprika by UHPLC-HRMS fingerprinting and
309 multivariate calibration methods (PCA and PLS-DA). *Foods*, 9, 1–10.
- 310 Barker, M., & Rayens, W. (2003). Partial least squares for discrimination. *Journal of*
311 *Chemometrics*, 17, 166–173.
- 312 Bonaccorsi, I., Cacciola, F., Utczas, M., Inferrera, V., Giuffrida, D., Donato, P., ...
313 Mondello, L. (2016). Characterization of the pigment fraction in sweet bell peppers
314 (*Capsicum annuum* L.) harvested at green and overripe yellow and red stages by
315 offline multidimensional convergence chromatography/liquid chromatography–
316 mass spectrometry. *Journal of Separation Science*, 39(17), 3281–3291.
317 <https://doi.org/10.1002/jssc.201600220>
- 318 Cetó, X., Sánchez, C., Serrano, N., Díaz-Cruz, J. M., & Núñez, O. (2020). Authentication
319 of paprika using HPLC-UV fingerprints. *LWT - Food Science and Technology*, 124,
320 109153.
- 321 Cuadros-Rodríguez, L., Valverde-Som, L., Jiménez-Carvelo, A. M., & Delgado-Aguilar,
322 M. (2020). Validation requirements of screening analytical methods based on
323 scenario-specified applicability indicators. *TrAC - Trends in Analytical Chemistry*,
324 122.
- 325 Hernández-Hierro, J. M., García-Villanova, R. J., & González-Martín, I. (2008). Potential
326 of near infrared spectroscopy for the analysis of mycotoxins applied to naturally
327 contaminated red paprika. *Analytica Chimica Acta*, 2, 189–194.
- 328 Hernández, A., Martín, A., Aranda, E., Bartolomé, T., & Córdoba, M. de G. (2007).
329 Application of temperature-induced phase partition of proteins for the detection of
330 smoked paprika adulteration by free zone capillary electrophoresis (FZCE). *Food*

331 *Chemistry*, 105, 1219–1227.

332 Ignat, T., Schmilovitch, Z., Fefoldi, J., Steiner, B., & Alkalai-Tuvia, S. (2012). Non-
333 destructive measurement of ascorbic acid content in bell peppers by VIS-NIR and
334 SWIR spectrometry. *Postharvest Biology and Technology*, 74, 91–99.

335 Ignat, Timea, Schmilovitch, Z., Feföldi, J., Bernstein, N., Steiner, B., Egozi, H., &
336 Hoffman, A. (2013). Nonlinear methods for estimation of maturity stage, total
337 chlorophyll, and carotenoid content in intact bell peppers. *Biosystems Engineering*,
338 114, 414–425.

339 Kim, E. H., Lee, S. Y., Baek, D. Y., Park, S. Y., Lee, S. G., Ryu, T. H., ... Oh, S. W.
340 (2019). A comparison of the nutrient composition and statistical profile in red pepper
341 fruits (*Capsicum annuum* L.) based on genetic and environmental factors. *Applied*
342 *Biological Chemistry*, (1), 62–48.

343 Kucharska-Ambrożej, K., & Karpinska, J. (2020). The application of spectroscopic
344 techniques in combination with chemometrics for detection adulteration of some
345 herbs and spices. *Microchemical Journal*, 153, 104278.

346 Lim, J., Kim, G., Mo, C., & Kim, M. (2015). Design and fabrication of a real-time
347 measurement system for the capsaicinoid content of Korean red pepper (*Capsicum*
348 *annuum* L.) powder by visible and Near-Infrared Spectroscopy. *Journal of*
349 *Biosystems Engineering*, 15, 47–60.

350 Martens, H., & Stark, E. (1991). Extended multiplicative signal correction and spectral
351 interference subtraction: New preprocessing methods for near infrared spectroscopy.
352 *Journal of Pharmaceutical and Biomedical Analysis*, 9(8), 625–635.

353 Martín, A., Hernández, A., Aranda, E., Casquete, R., Velázquez, R., Bartolomé, T., &
354 Córdoba, M. G. (2017). Impact of volatile composition on the sensorial attributes of
355 dried paprikas. *Food Research International*, 100, 691–697.

356 Mohanty, N., John, A. L. S., Manmatha, R., & Rath, T. M. (2013). Shape-based image
357 classification and retrieval. *Handbook of Statistics*, 31, 249–267.
358 <https://doi.org/10.1016/B978-0-444-53859-8.00010-2>

359 Molnár, H., Kónya, É., Zalán, Z., Bata-Vidács, I., Tömösközi-Farkas, R., Székács, A., &
360 Adányi, N. (2018). Chemical characteristics of spice paprika of different origins.
361 *Food Control*, 83, 54–60. <https://doi.org/10.1016/j.foodcont.2017.04.028>

362 Monago-Maraña, O., Galeano-Díaz, T., & Muñoz de la Peña, A. (2017). Chemometric
363 Discrimination Between Smoked and Non-Smoked Paprika Samples. Quantification
364 of PAHs in Smoked Paprika by Fluorescence-U-PLS/RBL. *Food Analytical*

365 *Methods*, 10, 1128–1137.

366 Monago Maraña, O., Bartolomé García, T. de J., & Galeano Díaz, T. (2016).
367 Characterization of Spanish Paprika by Multivariate Analysis of Absorption and
368 Fluorescence Spectra. *Analytical Letters*, 49, 1184–1197.

369 Moros, J., Llorca, I., Cervera, M. L., Pastor, A., Garrigues, S., & de la Guardia, M. (2008).
370 Chemometric determination of arsenic and lead in untreated powdered red paprika
371 by diffuse reflectance near-infrared spectroscopy. *Analytica Chimica Acta*, 613,
372 196–206.

373 Núñez-Sánchez, N., Martínez-Marín, A. L., Polvillo, O., Fernández-Cabanás, V. M.,
374 Carrizosa, J., Urrutia, B., & Serradilla, J. M. (2016). Near Infrared Spectroscopy
375 (NIRS) for the determination of the milk fat fatty acid profile of goats. *Food*
376 *Chemistry*, 190, 244–252.

377 Oliveira, M. M., Cruz-Tirado, J. P., Roque, J. V., Teófilo, R. F., & Barbin, D. F. (2020).
378 Portable near-infrared spectroscopy for rapid authentication of adulterated paprika
379 powder. *Journal of Food Composition and Analysis*, 87, 103403.

380 Oliveira, Marciano M., Cruz-Tirado, J. P., & Barbin, D. F. (2019). Nontargeted analytical
381 methods as a powerful tool for the authentication of spices and herbs: a review.
382 *Comprehensive Reviews in Food Science and Food Safety*, 18, 670–689.

383 Palacios-Morillo, A., Jurado, J. M., Alcázar, A., & Pablos, F. (2016). Differentiation of
384 Spanish paprika from Protected Designation of Origin based on color measurements
385 and pattern recognition. *Food Control*, 62, 243–249.

386 Palacios-Morillo, Ana, Jurado, J. M., Alcázar, Á., & De Pablos, F. (2014). Geographical
387 characterization of Spanish PDO paprika by multivariate analysis of multielemental
388 content. *Talanta*, 128, 15–22.

389 Park, T. S., Candidate, P. D., Bae, Y. M., Researcher, S., Sim, M. J., & Student, G. (2008).
390 Analysis of Capsaicinoids from Hot Red Pepper Powder by Near-Infrared
391 Spectroscopy. *ASABE Annual International Meeting*, (January 2008), 1–7.
392 <https://doi.org/10.13031/2013.25077>

393 Penchaiya, P., Bobelyn, E., Verlinden, B. E., Nicolai, B. M., & Saeys, W. (2009). Non-
394 destructive measurement of firmness and soluble solids content in bell pepper using
395 NIR spectroscopy. *Journal of Food Engineering*, 94, 267–273.

396 Pérez-Juan, M., Afseth, N. K., González, J., Díaz, I., Gispert, M., Furnols, M. F. i., ...
397 Realini, C. E. (2010). Prediction of fatty acid composition using a NIRS fibre optics
398 probe at two different locations of ham subcutaneous fat. *Food Research*

399 *International*, 43(5), 1416–1422.

400 Tharwat, A. (2016). Linear vs. quadratic discriminant analysis classifier: a tutorial.

401 *International Journal of Applied Pattern Recognition*, 3(2), 145.

402 <https://doi.org/10.1504/ijapr.2016.079050>

403 TR No 01/2015. (2015). *Guide to NMR Method Development and Validation – Part II :*

404 *Multivariate data analysis*.

405 Unión Europea, U. (2006). *Reglamento (CE) Nº 510/2006 del Consejo. S. Diario Oficial*

406 *de la Unión Europea* (Vol. C 287/2).

407 Wold, S., Esbensen, K. I. M., & Geladi, P. (1987). Principal Component Analysis.

408 *Chemometrics and Intelligent Laboratory Systems*, 2, 37–52.

409

410 **Figure captions**

411 **Figure 1.** (A) Average of absorption spectra (B) Average of EMSC pre-processed spectra. Black
412 lines correspond to the PDO samples and red lines correspond to the non-PDO samples.

413

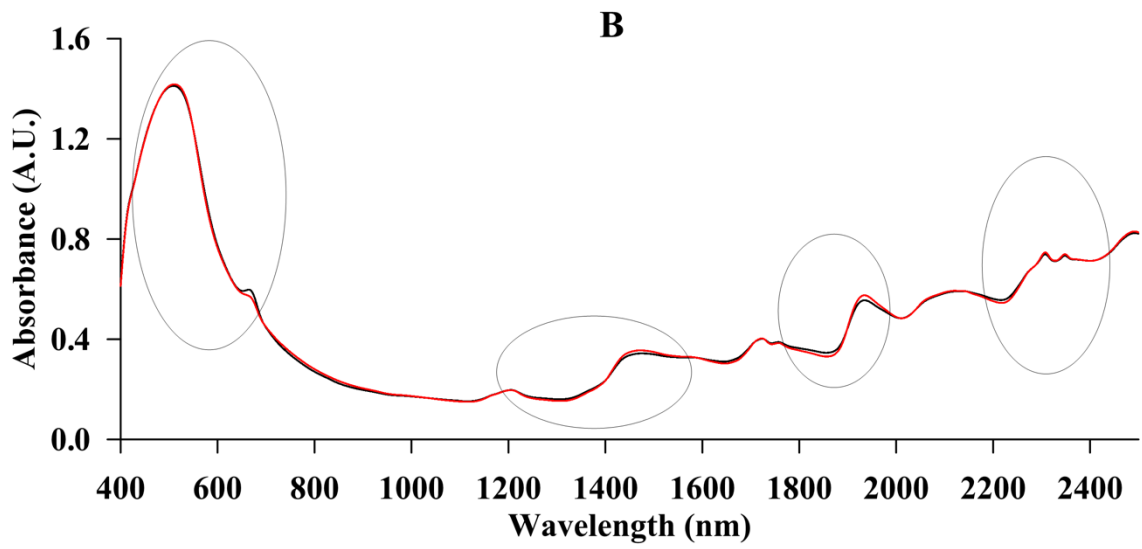
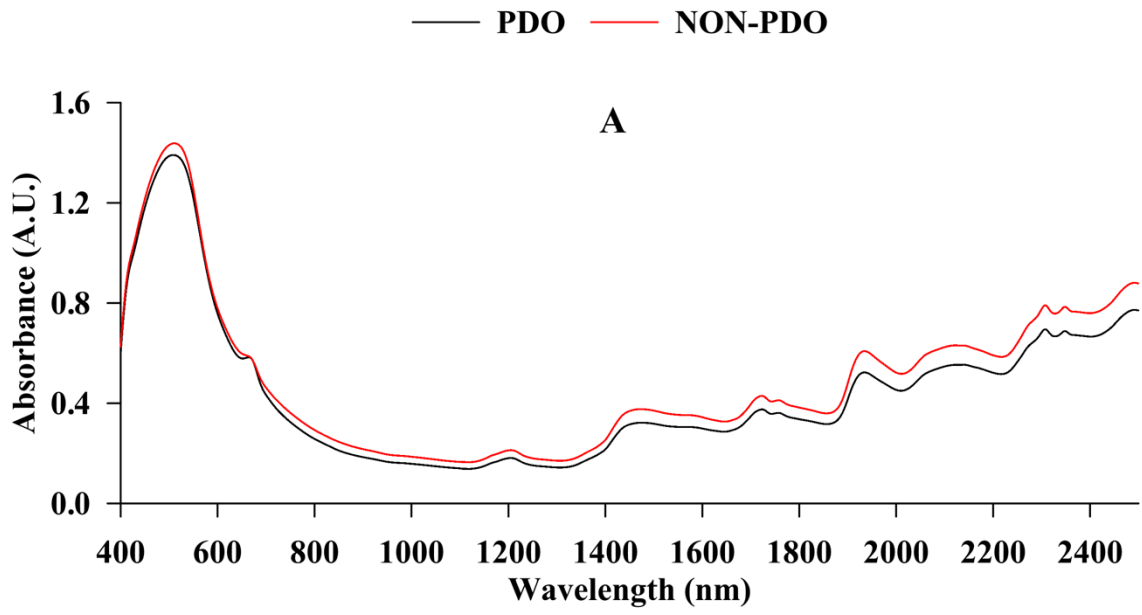
414 **Figure 2.** Loadings (B, D, F) and scores values (A, C, E) obtained from PCA of the spectra in
415 wavelength ranges: 400 - 2500 nm, 400 - 800 nm and 800 - 2500 nm.

416

417 **Figure 3.** Regression coefficients for non-PDO samples obtained for the PLS-DA models for the
418 different spectral ranges studied.

419

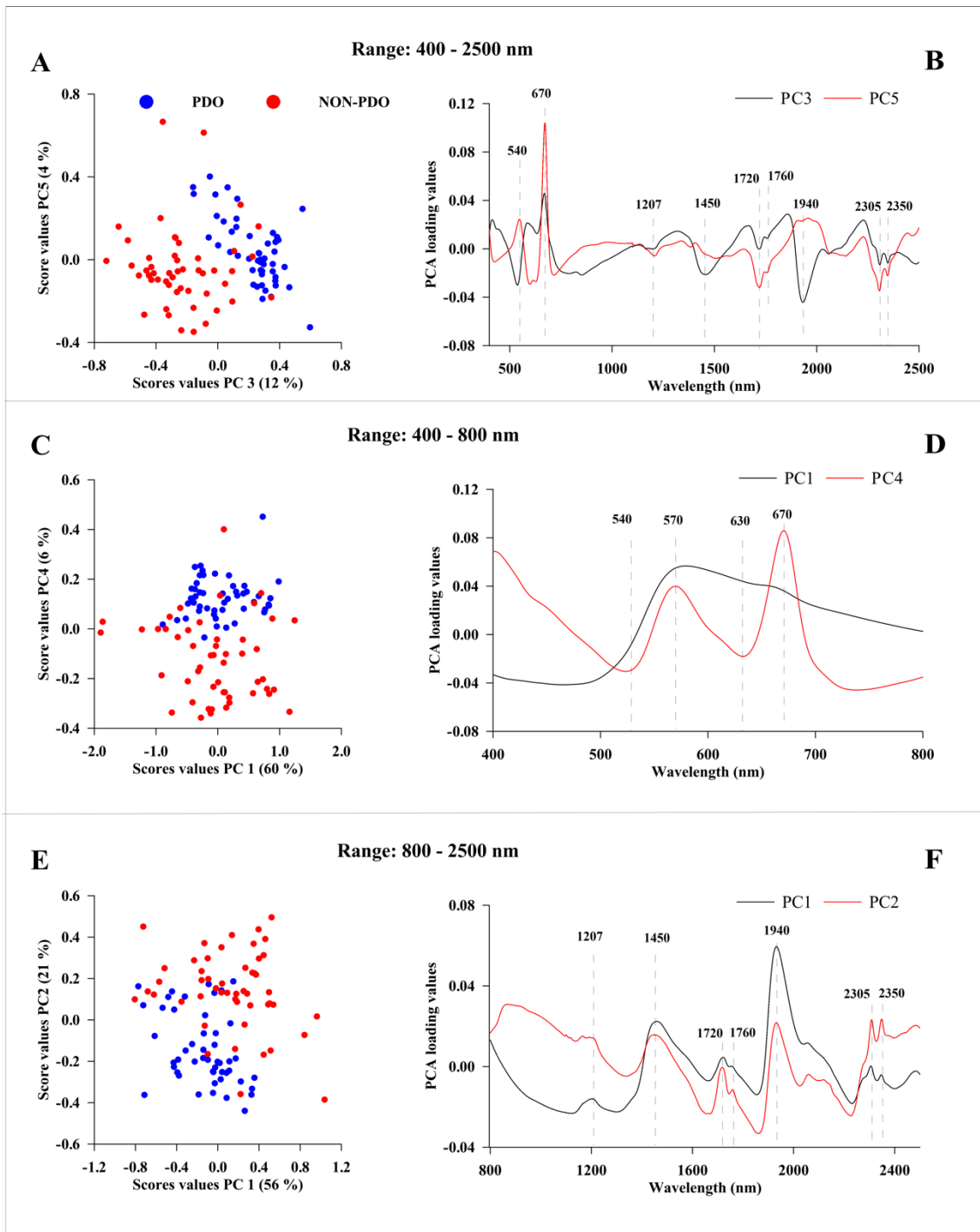
420



421

422

Figure 1

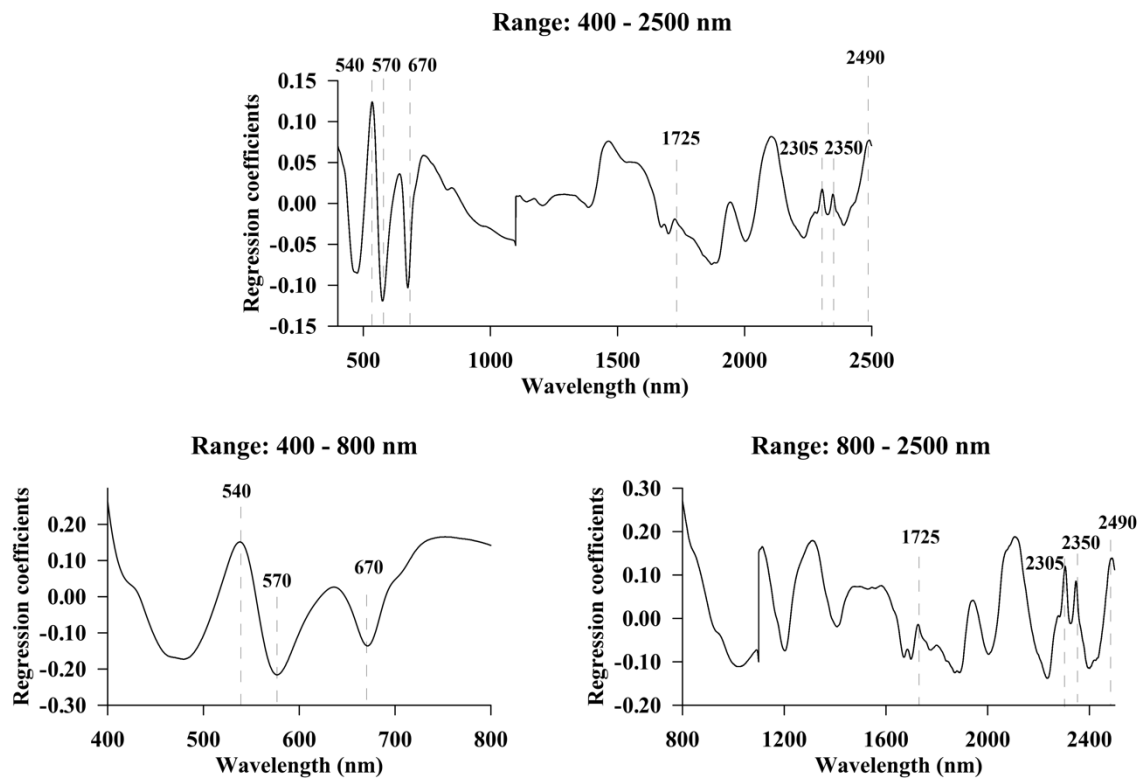


423

424

425

Figure 2



426

427

428

Figure 3

Table 1. Confusion matrices for the different algorithms and ranges studied in the training and test sets.

Algorithm	Range (nm)	N° comp	%EV (X)	Training set		Test set		
				PDO (CV)	NON- PDO (CV)	PDO (val)	NON-PDO (val)	
PLS-DA	400 - 2500	6	96 (1)	PDO	28 (1)	1 (1)	19 (1)	1 (1)
				NON-PDO	5 (3)	25 (3)	2 (2)	18 (2)
	400 - 800	5	99 (0)	PDO	28 (1)	1 (1)	19 (1)	1 (1)
				NON-PDO	6 (2)	24 (2)	3 (1)	17 (1)
	800 - 2500	6	98 (1)	PDO	28 (0)	1 (0)	19 (1)	1 (1)
				NON-PDO	3 (2)	27 (2)	1 (2)	19 (2)
PCA-LDA	400 - 2500	5	96 (0)	PDO	27 (1)	2 (1)	19 (1)	1 (1)
				NON-PDO	7 (2)	23 (2)	2 (2)	18 (2)
	400 - 800	5	99 (0)	PDO	28 (1)	1 (1)	19 (1)	1 (1)
				NON-PDO	6 (2)	24 (2)	3 (1)	17 (1)
	800 - 2500	5	98 (1)	PDO	25 (2)	4 (2)	17 (2)	3 (2)
				NON-PDO	5 (2)	25 (2)	2 (2)	18 (2)
PCA-QDA	400 - 2500	5	97 (1)	PDO	27 (1)	2 (1)	17 (2)	2 (2)
				NON-PDO	3 (1)	27 (1)	2 (2)	18 (2)
	400 - 800	5	99 (0)	PDO	26 (2)	3 (2)	18 (1)	2 (1)
				NON-PDO	3 (1)	27 (1)	2 (2)	18 (2)
	800 - 2500	5	96 (1)	PDO	26 (1)	3 (1)	16 (3)	4 (3)
				NON-PDO	2 (1)	28 (1)	2 (2)	18 (2)

*CV: cross-validation; numbers in parentheses correspond to the standard deviation of three sets assayed.

429

430

Table 2. Validation parameters calculated for the target class (PDO class) in the different classification methods.

Algorithm	Range (nm)	Training set							Test set						
		SPEC	SENS	PREC	ER	ACCUR	I _{ERROR}	I _{LOSS}	SPEC	SENS	PREC	ER	ACCUR	I _{ERROR}	I _{LOSS}
PLS-DA	400 - 2500	0.85 (0.11)	0.98 (0.02)	0.86 (0.09)	0.09 (0.06)	0.91 (0.06)	0.08 (0.05)	0.01 (0.05)	0.92 (0.10)	0.97 (0.03)	0.93 (0.09)	0.06 (0.06)	0.94 (0.05)	0.04 (0.05)	0.02 (0.01)
	400 - 800	0.81 (0.08)	0.97 (0.04)	0.83 (0.07)	0.11 (0.05)	0.89 (0.06)	0.10 (0.04)	0.02 (0.02)	0.87 (0.06)	0.97 (0.06)	0.88 (0.05)	0.08 (0.06)	0.92 (0.06)	0.07 (0.03)	0.02 (0.03)
	800 - 2500	0.90 (0.07)	0.97 (0.0)	0.91 (0.06)	0.07 (0.04)	0.93 (0.04)	0.05 (0.03)	0.02 (0.00)	0.93 (0.08)	0.97 (0.03)	0.94 (0.07)	0.05 (0.04)	0.95 (0.04)	0.03 (0.04)	0.02 (0.01)
PCA-LDA	400 - 2500	0.78 (0.07)	0.94 (0.02)	0.80 (0.05)	0.14 (0.04)	0.86 (0.04)	0.11 (0.03)	0.03 (0.00)	0.88 (0.08)	0.97 (0.06)	0.89 (0.06)	0.08 (0.04)	0.92 (0.04)	0.06 (0.04)	0.02 (0.03)
	400 - 800	0.80 (0.06)	0.97 (0.04)	0.82 (0.05)	0.12 (0.03)	0.88 (0.03)	0.10 (0.04)	0.02 (0.01)	0.87 (0.06)	0.97 (0.06)	0.88 (0.05)	0.08 (0.06)	0.92 (0.06)	0.07 (0.03)	0.02 (0.03)
	800 - 2500	0.82 (0.05)	0.87 (0.05)	0.82 (0.05)	0.15 (0.04)	0.85 (0.04)	0.09 (0.03)	0.04 (0.02)	0.90 (0.09)	0.87 (0.10)	0.90 (0.07)	0.12 (0.06)	0.88 (0.06)	0.05 (0.04)	0.07 (0.05)
PCA-QDA	400 - 2500	0.91 (0.02)	0.92 (0.02)	0.91 (0.02)	0.08 (0.01)	0.92 (0.00)	0.04 (0.01)	0.04 (0.01)	0.92 (0.08)	0.87 (0.10)	0.92 (0.07)	0.11 (0.02)	0.89 (0.01)	0.04 (0.04)	0.07 (0.05)
	400 - 800	0.90 (0.03)	0.89 (0.05)	0.90 (0.04)	0.11 (0.04)	0.89 (0.04)	0.04 (0.02)	0.05 (0.03)	0.92 (0.08)	0.90 (0.05)	0.92 (0.07)	0.09 (0.02)	0.91 (0.01)	0.05 (0.05)	0.06 (0.01)
	800 - 2500	0.92 (0.02)	0.90 (0.04)	0.92 (0.02)	0.09 (0.03)	0.91 (0.03)	0.04 (0.01)	0.05 (0.02)	0.92 (0.10)	0.78 (0.16)	0.92 (0.10)	0.15 (0.07)	0.85 (0.07)	0.04 (0.05)	0.11 (0.08)

Numbers in parentheses correspond to the standard deviation of three sets assayed.

431

432